MODELS FOR THE THERMODYNAMIC PROPERTIES, DENSITY AND VISCOSITY OF MOLTEN SALTS

Christian Robelin, Arthur Pelton, Patrice Chartrand & Gunnar Eriksson
École Polytechnique, Canada

ABSTRACT

Over the past several years, we have developed a quantitative thermodynamic description of multicomponent molten salt systems such as LiCl-NaCl-KCl-$MgCl_2$-$CaCl_2$-$MnCl_2$-$FeCl_2$-$FeCl_3$-$CoCl_2$-$NiCl_2$-$AlCl_3$ and NaF-AlF_3-CaF_2-Al_2O_3, using the Modified Quasichemical Model for short-range ordering. The model parameters are mainly obtained by the critical evaluation and optimization of available thermodynamic and phase equilibrium data for the binary and ternary subsystems. The model is then used to estimate the properties of multicomponent salts from these assessed binary and ternary parameters using interpolation methods. When used in conjunction with thermodynamic databases for solids, solid solutions, other liquid solutions (such as liquid metals), and gases, these databases permit the calculation of complex multiphase equilibria in multicomponent systems. Theoretical models based on the Modified Quasichemical Model were developed recently for the density and viscosity of multicomponent inorganic liquids, and were applied successfully to the NaCl-KCl-$MgCl_2$-$CaCl_2$ and NaF-AlF_3-CaF_2-Al_2O_3 electrolytes.

It is thus possible to calculate simultaneously the phase relations, thermodynamic properties, density and viscosity of multicomponent molten salts over wide composition and temperature ranges. These calculations are important for the understanding and control of the corresponding industrial processes, and can be performed with the FactSage thermochemical software.

In the present paper, the models developed for the thermodynamic properties, density and viscosity of multicomponent molten salts are illustrated with emphasis on the NaF-AlF_3-CaF_2-Al_2O_3 system.

INTRODUCTION

Molten chlorides and fluorides are involved in various industrial applications such as fluxes for metal treatment, and alumina reduction from cryolite-based electrolytes. Thermodynamic information (enthalpy of mixing, emf), phase equilibria (vapor pressures, liquidus temperatures) as well as information on properties such as molar volume (density), viscosity and electrical conductivity are important for the understanding and control of the corresponding processes.

Thermodynamic databases have been developed for the LiCl-NaCl-KCl-$MgCl_2$-$CaCl_2$-$MnCl_2$-$FeCl_2$-$FeCl_3$-$CoCl_2$-$NiCl_2$-$AlCl_3$ [1, 2, 3, 4, 5] and NaF-AlF_3-CaF_2-Al_2O_3 [6] systems. The molten chloride system was modeled using the Modified Quasichemical Model in the Pair Approximation [7, 8], which takes into account short-range ordering between second-nearest-neighbor cations. The NaF-AlF_3-CaF_2-Al_2O_3 liquid was modeled using the Modified Quasichemical Model in the Quadruplet Approximation [9] that evaluates coupled 1st-nearest-neighbor (cation/anion) and 2nd -nearest-neighbor (cation/cation and anion/anion) short-range order. (Each quadruplet is formed of two cations and two anions.)

A theoretical model based on the Modified Quasichemical Model was developed recently for the density of multicomponent inorganic liquids [10, 11, 12], and was applied successfully to liquid alloys (unpublished work), common-ion molten salt mixtures (NaCl-KCl-$MgCl_2$-$CaCl_2$ [11]) and reciprocal molten salt mixtures (NaF-AlF_3-CaF_2-Al_2O_3 [12]).

Finally, a viscosity model based both on the Modified Quasichemical Model and the density model was applied successfully to the NaCl-KCl-$MgCl_2$-$CaCl_2$ [13] and NaF-AlF_3-CaF_2-Al_2O_3 [10] liquids.

THERMODYNAMIC MODELS FOR THE LIQUID PHASES

The thermodynamic properties of the molten chloride system were modeled using the Modified Quasichemical Model in the Pair Approximation [7, 8]. Short-range ordering is treated by considering the relative numbers of second-nearest-neighbor cation–cation pairs, the only anion being Cl^-. The parameters of the model are the Gibbs free energy changes $\Delta g_{AB/Cl}$ for the following pair exchange reactions:

$$(A-Cl-A)_{pair} + (B-Cl-B)_{pair} = 2\,(A-Cl-B)_{pair} \qquad \Delta g_{AB/Cl} \tag{1}$$

where A and B are two different cations. As $\Delta g_{AB/Cl}$ becomes progressively more negative, reaction (1) is shifted to the right, (A–Cl–B) pairs predominate, and the solution becomes progressively more ordered. When $\Delta g_{AB/Cl}$ is small, the degree of short-range ordering is small, and the solution approximates a random (Bragg-Williams) mixture of cations on the cationic sublattice. Molten ACl-$AlCl_3$ solutions (where A = Li, Na and K) are well-known for exhibiting extensive short-range ordering near the equimolar composition. The existence of $AlCl_4^-$ and $Al_2Cl_7^-$ species in KCl-$AlCl_3$ melts was evidenced in particular by Raman spectroscopy [14, 15]. The Modified Quasichemical Model does not explicitly introduce complex anions. However, short-range ordering through reaction (1) when $\Delta g_{AB/Cl}$ is very negative yields a configurational entropy very similar to that obtained by the assumption of complex ions. For example, if the cation–cation coordination numbers of A^+ and Al^{3+} are set to be equal, and if $\Delta g_{AAl/Cl}$ is very negative, then, at the equimolar $AAlCl_4$ composition, the only second-nearest-neighbor cation-cation pairs are A-Cl-Al pairs (with negligible amounts of A-Cl-A and Al-Cl-Al pairs). That is, each Al^{3+} ion has four Cl^- ions in its first coordination shell, and only A^+ ions in its second coordination shell, as would be the case if the melt were formally considered as consisting of A^+ and

$AlCl_4^-$ ions. The main drawback of the explicit introduction of complex anions is that for multicomponent systems more complexes must be postulated and included in order to correctly represent the Gibbs energy of the liquid phase. Hence, the use of the present model permits large databases to be developed. Pure liquid aluminum chloride was modeled as a mixture of $AlCl_3$ and Al_2Cl_6 (i.e., as a mixture of Al^{3+}, Al_2^{6+} and Cl^- ions) in order to permit the definition of two different compositions of maximum short-range ordering (near the $AAlCl_4$ and AAl_2Cl_7 compositions) for the ACl-aluminum chloride binary systems (where A = Li, Na and K). This is consistent with the observation of $AlCl_4^-$ and $Al_2Cl_7^-$ *complex ions* in the ACl-aluminum chloride melts as discussed above.

The calculated NaCl-$AlCl_3$ phase diagram at 1 bar [2] is shown along with the available measurements in Figure 1.

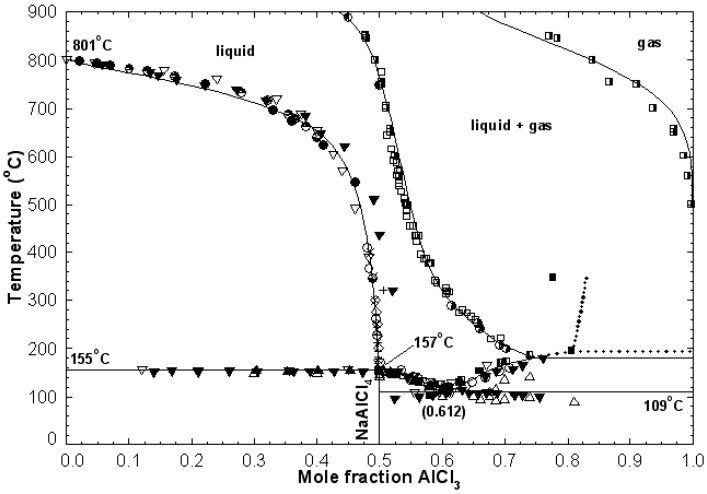

Figure 1: Calculated NaCl-$AlCl_3$ phase diagram at 1 bar (dotted lines are liquid-liquid miscibility gap boundary and monotectic at P > 1 bar). Reprinted from [2] with permission from Elsevier

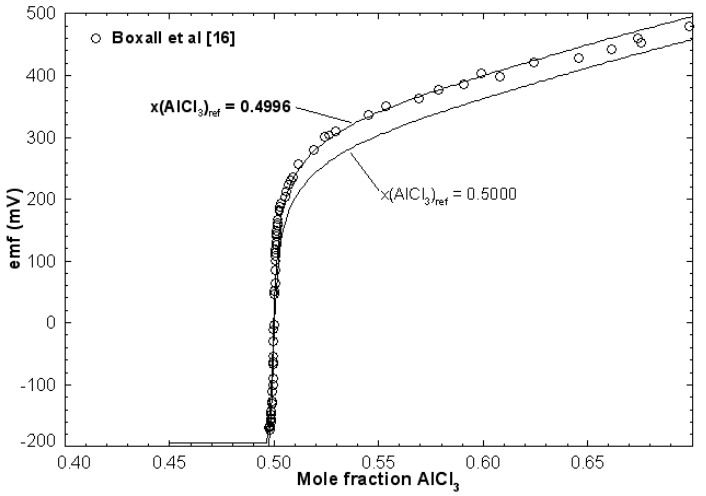

Figure 2: Calculated emf of the cell Al(s) / NaCl-$AlCl_3$(l) (ref) / fritted Pyrex / NaCl-$AlCl_3$(l) / Al(s) at 175°C, for two different compositions of the reference melt. Reprinted from [2] with permission from Elsevier

The calculated emf of the cell Al(s) | NaCl-$AlCl_3$(l) (ref.) | fritted pyrex | NaCl-$AlCl_3$(l) | Al(s) at 175˚C is compared to the measurements of Boxall *et al.* [16] in Figure 2. According to the authors, the reference melt had a constant composition close to equimolar. The best agreement between the calculated and experimental emf values was obtained for the composition $(X_{AlCl_3})_{ref}$ = 0.4996. Note that the calculated curve in Figure 2 is analogous to a classical titration curve.

The NaF-AlF_3-CaF_2-Al_2O_3 liquid solution consists of more than one cation and more than one anion. The thermodynamic properties of this reciprocal molten salt were modeled using the Modified Quasichemical Model in the Quadruplet Approximation [9]. In addition to the second-nearest-neighbor cation-cation pair exchange reactions defined by reaction (1) (with F^- instead of Cl^- as the common anion), one has to consider the following second-nearest-neighbor anion-anion pair exchange reactions:

$$(F-A-F)_{pair} + (O-A-O)_{pair} = 2\,(F-A-O)_{pair} \qquad \Delta g_{A/FO} \tag{2}$$

as well as the Gibbs energies of formation of the ABFO quadruplets from the binary quadruplets according to:

$$\tfrac{1}{2}\,(ABF_2 + ABO_2 + A_2FO + B_2FO) = 2\,(ABFO) \qquad \Delta g_{AB/FO} \tag{3}$$

where A and B are two different cations, and $\Delta g_{AB/FO}$ is expanded as an empirical polynomial in the mole fractions X_{A_2/F_2}, X_{A_2/O_2}, X_{B_2/F_2} and X_{B_2/O_2} of the A_2F_2, A_2O_2, B_2F_2 and B_2O_2 quadruplets [9].

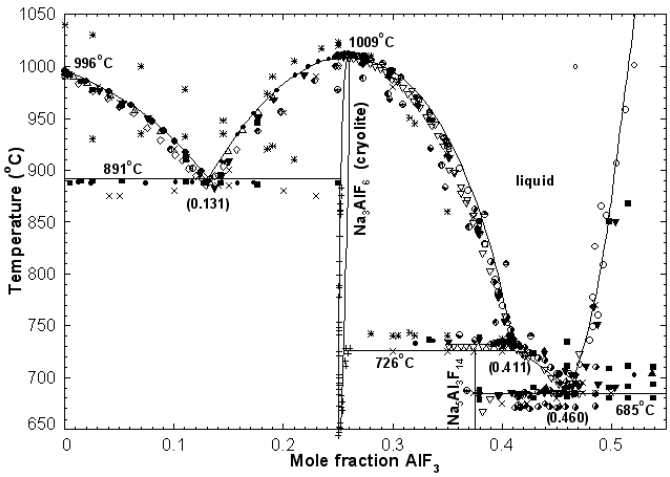

Figure 3: Calculated NaF-AlF_3 phase diagram. Reprinted from [6] with permission

The cations and anions considered in the liquid model are Na^+, Al_V^{3+}, Al_{IV}^{3+}, Al_2^{6+}, Ca^{2+} and F^-, O^{2-} respectively. Al_V^{3+} is 5-coordinated Al^{3+}, Al_{IV}^{3+} is 4-coordinated Al^{3+} and Al_2^{6+} represents dimerized (F-bridged) Al^{3+}. Pure (hypothetical) liquid aluminum fluoride was modeled as a mixture of Al_V^{3+}, Al_{IV}^{3+}, Al_2^{6+} and F^- ions in order to permit us to define three different compositions of maximum short-range ordering (near the Na_2AlF_5, $NaAlF_4$ and $NaAl_2F_7$ compositions) in the NaF-AlF_3 binary system. The existence of AlF_6^{3-}, AlF_5^{2-} and AlF_4^- *complex anions* in AF-AlF_3 melts (where A = Li, Na and K) has been evidenced in the literature by Raman spectroscopy [17, 18, 19, 20, 21]. The liquid model assumes that the

concentration of AlF_6^{3-} *complex anions* is negligible. In the NaF-AlF_3 binary system, a composition of maximum short-range ordering near the $NaAl_2F_7$ composition was introduced in order to reproduce satisfactorily the experimental liquidus of AlF_3, which is quite steep close to the equimolar composition.

The calculated NaF-AlF_3 phase diagram [6] is shown along with the available measurements in Figure 3. Accorded to Chrenkova *et al.* [22], the electrolyte used for aluminum production is typically (Na_3AlF_6 + 6-13 wt% AlF_3 + 3-8 wt% CaF_2 + 2-5 wt% Al_2O_3) and the operating temperature is 945-970°C. The calculated (*predicted*) Na_3AlF_6 and Al_2O_3 liquidus curves for the Na_3AlF_6-AlF_3-CaF_2-Al_2O_3 system with 10 wt% AlF_3 and 5 or 10 wt% CaF_2 are compared to the measurements of Fenerty and Hollingshead [23] in Figure 4. The data points in Figure 4 were not used to obtain the model parameters. That is, the liquidus lines in Figure 4 are predicted by the model solely from the model parameters obtained from optimization of the low-order subsystems.

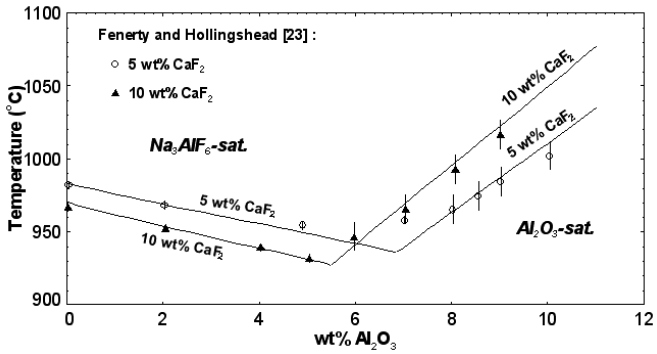

Figure 4 : Calculated (*predicted*) Na_3AlF_6 and Al_2O_3 liquidus curves for the Na_3AlF_6-AlF_3-CaF_2-Al_2O_3 system with 10 wt% AlF_3 and 5 or 10 wt% CaF_2

DENSITY MODEL

This model has been described in detail previously [10, 11, 12]. For a given liquid phase, the density is easily derived from the molar volume, defined as the pressure derivative of the molar Gibbs energy at fixed temperature and composition. Therefore, by introducing into the Gibbs energy equation of the phase temperature-dependent molar volume expressions (Equations 4 and 5) for the pure components and pressure-dependent excess parameters for the binary (and, if necessary, higher-order) subsystems (Equation 6), it is possible to reproduce, and eventually predict, the density of the multicomponent liquid using interpolation methods.

The molar volume of a pure liquid salt at temperature T is given by:

$$V_m^{salt}(T) = V_m^{salt}(T_{ref}) \cdot exp\left(\int_{T_{ref}}^{T} \alpha(T) \cdot dT \right) \quad (4)$$

where T_{ref} is a reference temperature (arbitrarily chosen) and $\alpha(T)$ is the thermal expansivity varying with temperature as:

$$\alpha(T) = a + bT + cT^{-1} + dT^{-2} \quad (5)$$

The Gibbs energy change $\Delta g_{AB/F}$ (reaction analogous to (1)) is now given by:

$$\Delta g_{AB/F} = \Delta g^{thermo}_{AB/F} + \Delta g^{P}_{AB/F} \cdot (P - 1) \quad (6)$$

where $\Delta g^{thermo}_{AB/F}$ is independent of the hydrostatic pressure P (in bar) and corresponds to the thermodynamic model, and $\Delta g^{P}_{AB/F}$ corresponds to the density model. Similar equations are used for $\Delta g_{A/FO}$ (reaction (2)) and $\Delta g_{AB/FO}$ (reaction (3)).

The calculated density of NaF-AlF_3 melts at 1000˚C, 1030˚C, 1050˚C, 1070˚C and 1100˚C [12] is shown in Figure 5 along with the available measurements. Figure 5 shows that the model gives satisfactory results over the industrially important composition range *CR* = 1.8-2.6 (*CR* is the Cryolite Ratio, defined as the NaF/AlF_3 molar ratio). The calculated (*predicted*) density of Na_3AlF_6-AlF_3-CaF_2-Al_2O_3 melts at constant weight ratio $Na_3AlF_6/AlF_3/CaF_2$ = 88/6/6 or 91/6/3, and at various temperatures, is shown in Figure 6 along with the measurements of Itoh and Nakamura [24]. The data points in Figure 6 were not used to obtain the model parameters. That is, the density curves in Figure 6 are predicted by the model solely from the model parameters obtained from optimization of the low-order subsystems.

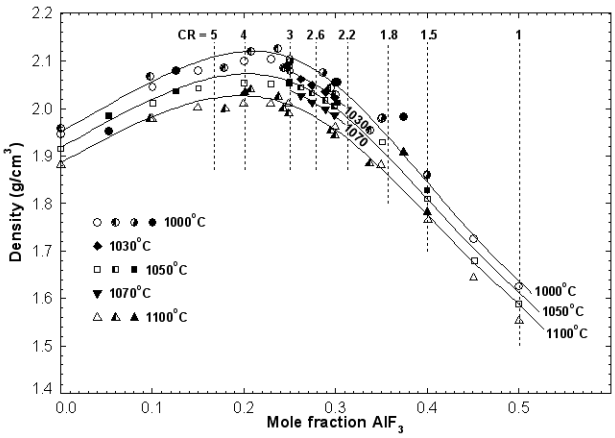

Figure 5 : Calculated density of NaF-AlF_3 melts at 1000ºC, 1030ºC, 1050ºC, 1070ºC and 1100ºC. Reprinted from [12] with permission from Springer Science and Business Media

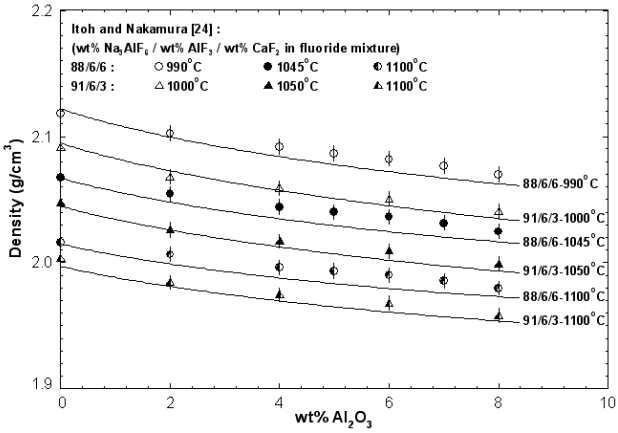

Figure 6: Calculated (*predicted*) density of Na_3AlF_6-AlF_3-CaF_2-Al_2O_3 melts at constant weight ratio $Na_3AlF_6/AlF_3/CaF_2$ = 88/6/6 or 91/6/3, and at various temperatures. Reprinted from [12] with permission from Springer Science and Business Media

The calculated (*predicted*) iso-density curves at 960˚C for NaF-AlF_3-CaF_2-Al_2O_3 melts with 5 wt% CaF_2 are shown in Figure 7 for various *CR* and various wt% Al_2O_3. (The iso-density curves are only drawn in the region of composition where no solid phase precipitates.) As mentioned previously [12], the density model gives less satisfactory results for very acidic (*i.e., CR* < 1.50) NaF-AlF_3 melts. Therefore, the predicted iso-density curves in Figure 7 may be less reliable for *CR* < 1.50.

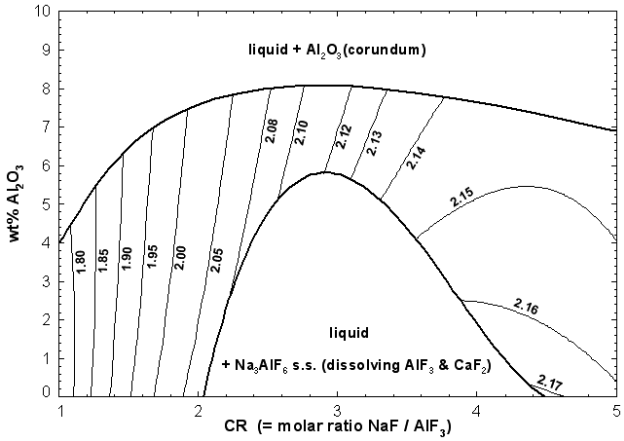

Figure 7: Calculated (*predicted*) iso-density (g/cm^3) curves at 960ºC for NaF-AlF_3-CaF_2-Al_2O_3 melts with 5 wt% CaF_2

VISCOSITY MODEL

This model has been described previously [10, 13]. The viscosity of the NaCl-KCl-$MgCl_2$-$CaCl_2$ [13] (respectively NaF-AlF_3-CaF_2-Al_2O_3 [10]) liquid was modeled using the following Eyring-type Equation [25]:

$$\eta = \frac{hN_{Av}}{V_m}\exp\left(\frac{G^*}{RT}\right) \quad \text{with} \quad G^* = \sum_{pairs/quad.} X_{pair/quad.}\left(A_{pair/quad.} + B_{pair/quad.}T\right) \qquad (7)$$

where h is Planck's constant, N_{Av} is Avogadro's number, V_m is the molar volume of the liquid (calculated from the density model), is the gas constant, G^* is a molar viscous activation energy expanded as a 1st-order polynomial in the second-nearest-neighbor cation-cation pair (or quadruplet) mole fractions $X_{pair/quad.}$, and $A_{pair/quad.}$ and $B_{pair/quad.}$ are model parameters.

The pairs/quadruplets may be regarded as structural units and can be calculated from the thermodynamic model at a given temperature, pressure and (global) composition. Expanding G^* in terms of the concentrations of structural units as in Equation 7, rather than in terms of the component mole fractions, results in better predictions of viscosities.

The calculated viscosity of NaF-AlF_3 melts for various mole fractions of AlF_3 is shown in Figures 8 and 9 along with the measurements of Brockner *et al.* [26], Silny *et al.* [27] and Fellner and Silny [28].

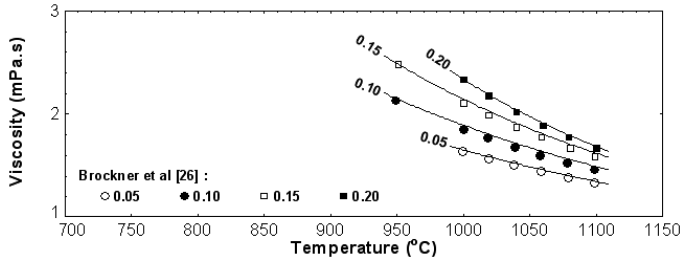

Figure 8: Calculated viscosity of NaF-AlF_3 melts for various mole fractions of AlF_3.
Reprinted from [10] with permission

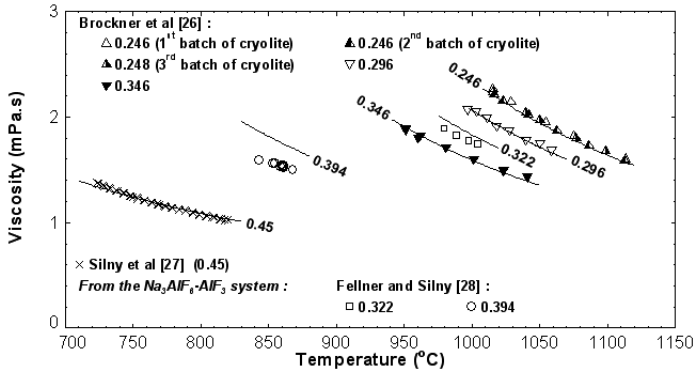

Figure 9: Calculated viscosity of NaF-AlF_3 melts for various mole fractions of AlF_3 (...).
Reprinted from [10] with permission

The calculated viscosities at 1000˚C and 1100˚C of NaF-AlF_3-CaF_2-Al_2O_3 melts with *BR* = 1.17 or 1.50, 5 wt% CaF_2 and 7.6 wt% Al_2O_3 are compared to the measurements of Hertzberg *et al.* [29] in Table 1. (*BR* is the Bath Ratio, defined as the NaF/AlF_3 weight ratio.)

Table 1 : Calculated and experimental [29] viscosities of NaF-AlF_3-CaF_2-Al_2O_3 melts with *BR* = 1.17 or 1.50, 5 wt% CaF_2 and 7.6 wt% Al_2O_3. Reprinted from [10] with permission

BR	Temperature (°C)	Experimental viscosity (mPa.s)	Calculated viscosity (mPa.s)	Shift (%)
1.17	1000	2.661	2.570	-3.42
	1100	1.854	1.909	2.97
1.50	1000	2.877	2.968	3.16
	1100	2.023	2.158	6.67

The calculated (*predicted*) iso-viscosity curves at 960˚C for NaF-AlF_3-CaF_2-Al_2O_3 melts with 5 wt% CaF_2 are shown in Figure 10 for various *CR* and various wt% Al_2O_3. (The iso-viscosity curves are only drawn in the region of composition where no solid phase precipitates).

To our knowledge, this is the first time that the viscosity of NaF-AlF_3-CaF_2-Al_2O_3 melts has been modeled. The viscosity model of Hertzberg *et al.* [29] was limited to the NaF-AlF_3-Al_2O_3 system.

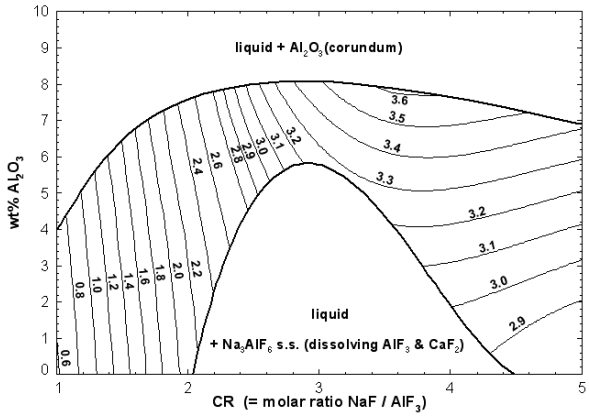

Figure 10: Calculated (*predicted*) iso-viscosity (mPa.s) curves at 960°C for NaF-AlF_3-CaF_2-Al_2O_3 melts with 5 wt% CaF_2

CONCLUSIONS

Over the past several years, thermodynamic databases have been developed for multicomponent molten salt systems such as LiCl-NaCl-KCl-$MgCl_2$-$CaCl_2$-$MnCl_2$-$FeCl_2$-$FeCl_3$-$CoCl_2$-$NiCl_2$-$AlCl_3$ [1, 2, 3, 4, 5] and NaF-AlF_3-CaF_2-Al_2O_3 [6], using the Modified Quasichemical Model for short-range ordering [7, 8, 9]. A theoretical model based on the Modified Quasichemical Model was developed recently for the density of multicomponent inorganic liquids [10, 11, 12] such as liquid alloys (unpublished work) and molten salts. The density of a given multicomponent molten salt can be modeled by fitting the temperature-dependent molar volumes of the pure liquid salts (Equations 4 and 5) and by introducing pressure-dependent parameters in the relevant Gibbs energy changes (reactions (1-3)). Finally, a viscosity model linked both to the Modified Quasichemical Model (through the calculated pair/quadruplet mole fractions) and to the density model (through the calculated molar volume) was applied successfully to common-ion molten salt mixtures [13] and reciprocal molten salt mixtures [10].

In the present article, the models developed for the thermodynamic properties, density and viscosity of multicomponent molten salts have been illustrated, with emphasis on the NaF-AlF_3-CaF_2-Al_2O_3 base electrolyte used for the electroreduction of alumina in Hall-Héroult cells. These various models are suitable for the development of databases for large systems. For each of these models, the parameters are obtained mainly by the critical evaluation and optimization of available data for the low-order (mostly binary and ternary) subsystems. The model is then able to use these assessed parameters for the low-order subsystems to predict the properties (thermodynamic properties and phase equilibria, density or viscosity) of the multicomponent system.

The optimized model parameters form databases for use with the FactSage thermochemical software [30].

ACKNOWLEDGEMENTS

This project was supported by two CRD grants from the Natural Sciences and Engineering Research Council of Canada in collaboration with the following companies: Alcoa, Hydro Aluminium, Rio Tinto-Alcan, INCO, Noranda, Rio Tinto, Teck Cominco, Dupont, Shell, Corning, Sintef, Schott Glas, St.-Gobain Recherche, Mintek and IIS Materials.

REFERENCES

Chartrand, P. & Pelton, A. D. (2001). Metall. Mater. Trans., 32A, pp. 1361-83. [1]

Robelin, C., Chartrand, P. & Pelton, A. D. (2004). J. Chem. Thermodyn., 36(8), pp. 683-99. [2]

Robelin, C., Chartrand, P. & Pelton, A. D. (2004). J. Chem. Thermodyn., 36(9), pp. 793-808. [3]

Robelin, C., Chartrand, P. & Pelton, A. D. (2004). J. Chem. Thermodyn., 36(9), pp. 809-28. [4]

Robelin, C., Chartrand, P. & Pelton, A. D. (2006). Proc. Electrochem. Soc., Molten Salts XIV, pp. 108-21. [5]

Chartrand, P. & Pelton A. D. (2002). Light Metals (Warrendale, PA), pp. 245-52. [6]

Pelton, A. D., Degterov, S. A., Eriksson, G., Robelin, C. & Dessureault, Y. (2000). Metall. Mater. Trans., 31B, pp. 651-9. [7]

Pelton, A. D. & Chartrand, P. (2001). Metall. Mater. Trans., 32A, pp. 1355-60. [8]

Pelton, A. D., Chartrand, P. & Eriksson, G. (2001). Metall. Mater. Trans., 32A, pp. 1409-16. [9]

Robelin, C. & Chartrand, P. (2007). Light Metals (Warrendale, PA), pp. 565-70. [10]

Robelin, C., Chartrand, P. & Eriksson, G. (2007). Metall. Mater. Trans., 38B, pp. 869-79. [11]

Robelin, C. & Chartrand, P. (2007). Metall. Mater. Trans., 38B, pp. 881-92. [12]

Mizani, S. (2008). Master's Thesis, Ecole Polytechnique, Montréal. [13]

Cyvin, S. J., Klaeboe, P., Rytter, E. & Øye, H. A. (1970). J. Chem. Phys., 52(5), pp. 2776-8. [14]

Øye, H. A., Rytter, E., Klaeboe, P. & Cyvin, S. J. (1971). Acta Chem. Scand., 25(2), pp. 559-76. [15]

Boxall, L. G., Jones, H. L. & Osteryoung, R. A. (1973). J. Electrochem. Soc., 120(2), pp. 223-1. [16]

Gilbert, B. & Materne, T. (1990). Appl. Spectr., 44(2), pp. 299-305. [17]

Tixhon, E., Robert, E. & Gilbert, B. (1994). Appl. Spectr., 48(12), pp. 1477-82. [18]

Gilbert, B., Robert, E., Tixhon, E., Olsen, J. E. & Østvold, T. (1995). Light Metals (Warrendale, PA), pp. 181-94. [19]

Gilbert, B., Robert, E., Tixhon, E., Olsen, J. E. & Østvold, T. (1996). Inorg. Chem., 35 (14), pp. 4198-4210. [20]

Robert, E., Olsen, J. E., Danek, V., Tixhon, E., Østvold, T. & Gilbert, B. (1997). J. Phys. Chem. B, 101(46), pp. 9447-57. [21]

Chrenkova, M., Danek, V., Silny, A. & Utigard, T. A. (1996). Light Metals (Warrendale, PA), pp. 227-32. [22]

Fenerty, A. & Hollingshead, E. A. (1960). J. Electrochem. Soc., 107(12), pp. 993-7. [23]

Itoh, K. & Nakamura, E. (1993). Sumitomo Keikinzoku Giho, 34(3), pp. 147-55. [24]

Glasstone, S., Laidler, K. J. & Eyring, H. (1941). *The Theory of Rate Processes – The Kinetics of Chemical Reactions, Viscosity, Diffusion and Electrochemical Phenomena.* McGraw-Hill Book Company Inc., New York & London, pp. 480-4. [25]

Brockner, W., Torklep, K. & Øye, H. A. (1979). Ber. Bunsenges. Phys. Chem., 83(1), pp. 12-19. [26]

Silny, A., Chrenkova, M., Danek, V., Vasiljev, R., Nguyen, D. K. & Thonstad, J. (2004). J.Chem. Eng. Data, 49(6), pp. 1542-5. [27]

Fellner, P. & Silny, A. (1994). Ber. Bunsenges. Phys. Chem., 98(7), pp. 935-7. [28]

Hertzberg, T., Torklep, K. & Øye, H. A. (1980). Light Metals, pp. 159-70. [29]

Bale, C. W., Chartrand, P., Degterov, S. A., Eriksson, G., Hack, K., Ben Mahfoud, R., Melançon, J., Pelton, A. D. & Petersen, S. (2002). CALPHAD, 26(2), pp. 189-228. [30]